Symbolic Dynamics of Coupled Map Lattices

Shawn D. Pethel,[1] Ned J. Corron,[1] and Erik Bollt[2]
[1]U.S. Army Aviation and Missile Command, AMSRD-AMR-WS-ST, Redstone Arsenal, Alabama 35898, USA
[2]Department of Math and Computer Science, Clarkson University, Potsdam, New York 13699-5805, USA
(Received 28 February 2005; published 27 January 2006)

We present a method to reduce the $\mathbb{R}^N$ dynamics of coupled map lattices (CMLs) of N invertibly coupled unimodal maps to a sequence of N-bit symbols. We claim that the symbolic description is complete and provides for the identification of all fixed points, periodic orbits, and dense orbits as well as an efficient representation for studying pattern formation in CMLs. We give our results for CMLs in terms of symbolic dynamical concepts well known for one-dimensional chaotic maps, including generating partitions, Gray orderings, and kneading sequences. An example utilizing coupled quadratic maps is given.

DOI: 10.1103/PhysRevLett.96.034105 PACS numbers: 05.45.Jn, 05.45.Ra

The study of complex motion is greatly simplified by investigating models that employ a coarse space-time discretization. Such models, typified by coupled map lattices (CMLs), have been shown to reproduce the essential features of turbulence in physical, chemical, and biological systems [1]. A further simplification can be achieved by considering iterates of the resulting map through a partition which reduces the chaotic motion to a purely symbolic signal with associated transition rules. The study of such signals is called *symbolic dynamics* [2]. An effective state-space-time discretization connects dynamical systems theory to the study of formal languages, and hence, to computer science, information theory, and automata [3]. Symbolic dynamical methods have been studied as a possible way to understand space-time chaos [4] and have recently been used [5] to bound entropy and determine ergodic properties of CMLs [6]. These attempts rely on specially constructed CMLs or on showing that Markov partitions of local, uncoupled dynamics are preserved in the presence of weak interactions [7,8].

In this Letter we describe the symbolic dynamics due to generating partitions, which we claim exist in a much broader class of CMLs, including those with strong coupling. For CMLs of N unimodal maps the implication is that evolution through the $\mathbb{R}^N$ state space is reducible to a sequence of N-bit symbols. We conjecture that the symbolic description is complete and provides for the rigorous identification of all fixed points, periodic orbits, and dense orbits as well as an efficient representation for studying pattern formation in CMLs [9]. We also show that the symbol ordering properties of 1D maps extend naturally to CMLs and allow the calculation of topological features without the need for extensive time series data. Importantly, the results presented here make straightforward the application to CMLs of symbolic dynamical methods used recently for the targeting and control of chaos [10–12], for probing the limits of synchronization [13], and for efficient chaos communication schemes [14–16].

We consider a map lattice with N sites labeled $i = 1, \ldots, N$. Each site is described by a state x_n^i in the interval $I = [a, b]$ and with local dynamics f_i: $I \to I$. A typical diffusively coupled map lattice (CML) as introduced by Kaneko is written as

$$x_{n+1}^i = (1 - \epsilon) f_i(x_n^i) + \epsilon/2[f_{i-1}(x_n^{i-1}) + f_{i+1}(x_n^{i+1})], \tag{1}$$

along with rules for the boundary sites [17]. The behavior of the lattice with respect to the coupling parameter ϵ is of primary interest here; the dynamics of the local maps f_i are well understood. In particular, we choose f with a good symbolic representation.

Such a function can be taken from the family of unimodal (single-humped) maps over the interval. We label the location of the maxima as the critical point x_c and divide the interval into two sets $\mathcal{P} = \{P_0, P_1\}$, where $P_0 = [a, x_c)$ and $P_1 = (x_c, b]$. The point $x_0 \in I$ is mapped to the semi-infinite symbol sequence $\pi(x_0) = \mathbf{s} = s_0 s_1 s_2 s_3 \ldots$ where

$$s_n = \begin{cases} 0 & \text{if } f^n(x_0) \in P_0, \\ 1 & \text{if } f^n(x_0) \in P_1. \end{cases} \tag{2}$$

The critical point can be assigned either symbol. In this formulation the dynamics are characterized by a set of rules that determine which sequences are allowed by f. The set of allowable sequences can be related to the state space through the inverse mapping

$$r(\mathbf{s}) = \bigcap_{n=0}^{\infty} f^{-n}(P_{s_n}). \tag{3}$$

For a faithful representation of chaotic dynamics, we require that $r(\mathbf{s})$ converge to a single point in the interval, or to the null set if $\mathbf{s}$ is not permitted by f. A partition that satisfies this property is referred to as *generating*. Note that for noninvertible maps f^{-1} has multiple solutions, one on each monotonic segment of f. For a partition to be generating each of these branches must be uniquely labeled, otherwise points that share a common image would not be distinguishable in sequence space.

 © 2006 The American Physical Society

Returning to the CML, denote by F the product function of f_i onto each site, and by A an $N \times N$ coupling matrix. Then (1) can be generalized as the composition $H = A \circ F$, where A is chosen consistent with H: $I^N \to I^N$. Assuming A is nonsingular, the elements of H^{-1} are

$$[H^{-1}(\mathbf{x}_0)]_i = f_i^{-1}\left(\sum_j A_{ij}^{-1} x_0^j\right), \tag{4}$$

keeping in mind that f_i^{-1} is multivalued. Because f_i^{-1} acts alone on the ith element the associated generating partition $\mathcal{P}^i$ of the solitary map f_i suffices to distinguish the branches of H_i^{-1}. Accordingly, we propose a partition for the CML that is the product of the partitions of the local maps. More precisely,

$$\mathcal{P}_{\mathrm{CML}} = \bigvee_{i=1}^{N} \mathcal{P}^i = \mathcal{P}^1 \vee \mathcal{P}^2 \vee \ldots \vee \mathcal{P}^N, \tag{5}$$

where $\mathcal{P} \vee \mathcal{P}' = \{P_k \cap P'_l\colon 0 \le k \le |\mathcal{P}| - 1, 0 \le l \le |\mathcal{P}'| - 1\}$ is the mathematical *join* of $\mathcal{P}$ and $\mathcal{P}'$. The form of (4) implies that the preimages of $H(\mathbf{x}_0)$ are uniquely labeled under this choice of partition. We conjecture, then, that $\mathcal{P}_{\mathrm{CML}}$ is generating for chaotic behavior in the CML. Our reasoning is that if the ergodicity is preserved by the coupling then the set of preimages $\{H^{-n}(\mathbf{x_0})\colon n \in \mathbb{N}\}$, each labeled differently under $\mathcal{P}_{\mathrm{CML}}$, covers the chaotic attractor and thus no two points on the attractor can be represented by the same semi-infinite symbol sequence.

In the case where all f_i are unimodal, the I^N state space can be coarsely discretized into 2^N regions without incurring a loss of fine detail on the attractor. As an example, consider the 2-element lattice H: $I^2 \to I^2$ written as

$$\begin{aligned} x_{n+1}^1 &= (1-\epsilon) f(x_n^1) + \epsilon f(x_n^2), \\ x_{n+1}^2 &= \epsilon f(x_n^1) + (1-\epsilon) f(x_n^2), \end{aligned} \tag{6}$$

where $f(x) = 1 - 2x^2$ is the quadratic map on the interval $I = [-1, 1]$. The quadratic map has a generating partition consisting of the regions $[-1, 0)$ and $(0, 1]$ which we shall denote as $\{P_0^1, P_1^1\}$, respectively, for coordinate x^1, and as $\{P_0^2, P_1^2\}$ for x^2. Applying (5) the partition for the coupled system is

$$\begin{aligned} \mathcal{P}_{\mathrm{CML}} &= \mathcal{P}^2 \vee \mathcal{P}^1 \\ &= \{P_0^2 \cap P_0^1, P_0^2 \cap P_1^1, P_1^2 \cap P_0^1, P_1^2 \cap P_1^1\}. \end{aligned} \tag{7}$$

Reading the subscripts of each term as a binary number, we relabel the regions as $\{P_0, P_1, P_2, P_3\}$ and assign to them the symbols 0, 1, 2, and 3. These four quadrants of I^2 are illustrated in Fig. 1(a).

The interesting dynamics of (6) occur for $\epsilon \in [0, 0.5]$. When the coupling is very strong ($0.25 < \epsilon \le 0.5$) the synchronization manifold is stable and the long-term behavior is that of a solitary quadratic map, for which $\mathcal{P}_{\mathrm{CML}}$ is known to be generating. At weaker coupling strengths

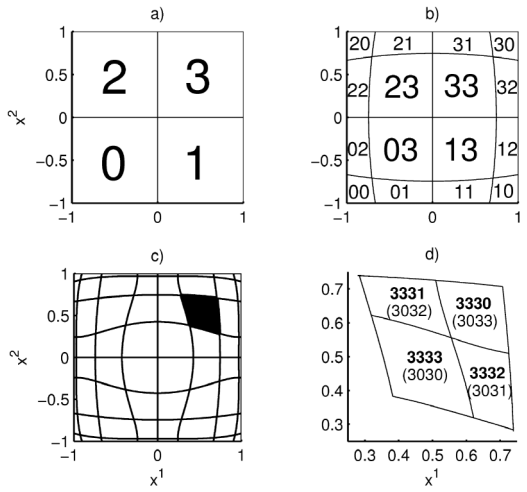

FIG. 1. Refinements of the square under a two element quadratic map lattice, Eq. (6), with coupling strength $\epsilon = 0.1$. (a) The primary partitioning of the square into four symbols, (b) the second refinement into 2-block sequences, (c) 3-block sequences (unlabeled) with region 313 darkened, and (d) region 313 subdivided into its 4-block words. The equivalent sequences under the inverse Gray transformation are shown parenthetically.

the dynamics are considerably more complicated. Empirically, a positive Lyapunov exponent in this regime indicates that the map is asymptotically expanding along typical orbits and thus the inverse mapping (3) converges to a set of zero measure. Figure 1 illustrates the refining of I^2 into increasingly smaller regions for $\epsilon = 0.1$. When this process is extended indefinitely, every point on the attractor is assigned a different symbol sequence.

The most powerful feature of the symbolic picture is that time evolution is reduced to a simple shift in sequence space. We denote the shift operator as σ and define its action on a symbol sequence as $\sigma(s_0 s_1 s_2 \ldots) = s_1 s_2 s_3 \ldots$, so that the effect of σ is to discard the leading symbol. If we set $\mathbf{s} = \pi(\mathbf{x_0})$, then it follows from (2) that $\sigma^n(\mathbf{s}) = \pi(\mathbf{x_n})$. Consequently, the entire evolution of $\mathbf{x_0}$ is contained in its symbolic representation. A point on a period-m orbit, for example, is conjugate to a sequence formed by infinitely repeating m symbols, or m *blocks*. This property has application in describing the spatiotemporal patterns that are observed in large CMLs [9]. A static or repeating global pattern would be represented by an eventually stationary or eventually periodic symbolic sequence. Spatially localized structures, such as traveling waves, appear in the bitwise decomposition of the symbols. In all cases, spatiotemporal patterns are more efficiently identified symbolically versus an analysis of real-valued CML states. In what follows we will describe a method for determining which symbol sequences are compatible with the dynamics of H and which sequences are forbidden due to dynamical restrictions.

In unimodal maps the symbolic sequence associated with the image of the critical point, referred to as the

kneading sequence, plays a special role in determining the admissibility of all other sequences [18–21]. When interpreted as a Gray code [22], the kneading sequence is the largest of all allowable sequences. Any sequence that orders above the kneading sequence is forbidden while those that order below it are admissible provided they do not contain sub-blocks that are inadmissible. The order of a sequence can be found by applying an inverse Gray transformation, G^{-1}, and interpreting the result as binary number. Given a symbol sequence $\mathbf{s} = s_1 s_2 s_3 \ldots, s_n \in \{0, 1\}$, the bitwise elements of $G^{-1}(\mathbf{s})$, denoted $b_1 b_2 b_3 \ldots$, are determined by setting $b_1 = s_1$ and

$$b_i = b_{i-1} \otimes s_i, \qquad \text{for } i > 1, \tag{8}$$

where $\otimes$ is the *exclusive*-OR operator.

To accommodate lattices of N elements, we apply the Gray transformation by defining the $\otimes$ operator to act bitwise on the N-bit representation of the symbols. For example: $2 \otimes 3 = 10 \otimes 11 = 01 = 1$. Thus the word 313 is mapped by (8) to 321 via the steps $b_1 = 3$, $b_2 = 3 \otimes 1 = 2$, and $b_3 = 3 \otimes 1 \otimes 3 = 1$. Like the 1D case, applying G^{-1} onto the symbol sequences produced by N coupled unimodal maps gives information about their relative location in state space. In this notation the subregion labels appear in the same spatial relationship as they do in the primary partitioning: for $N = 2$ the lower left ''quad'' of region 321 is labeled 3210, the lower right quad is 3211 and so on [see Fig. 1(d)].

In the CML the critical point is generalized to a critical surface of dimension $N - 1$, which is comprised of the generating partition boundaries. The image of the critical surface produces the associated kneading surface that bounds the attractor [23]. In Fig. 2(a) the kneading curve is the diamond shape. The symbolic sequences associated with this kneading curve are maximal in the sense that all sequences that lie outside of the region it encloses are forbidden. In this aspect, we have a partial order, and our work has a strong relationship to previous work [24] as a type of high-dimensional pruning front.

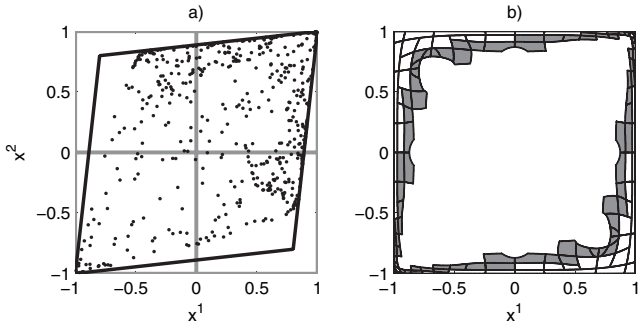

FIG. 2. The image of the critical curve and its fifth refinement for $\epsilon = 0.1$. (a) The kneading curve (heavy black lines) is comprised of the images of the generating partition boundaries (gray). The chaotic attractor, represented by 500 points, lies within this curve. (b) Here the kneading curve is shown as its fifth refinement by the gray-shaded regions. The area outside the kneading curve is tiled in by the 3-, 4-, and 5-block forbidden regions listed in Table I.

An algorithm for finding m-block forbidden sequences can be arrived at by comparing consecutive refinements of the kneading curve. Consider the set comprised of all the m-block subregions of the $(m-1)$th refinement of the kneading curve. The members of this set that lie strictly outside the mth refinement of the kneading curve are the m-block forbidden words. As in the case of unimodal maps, the inverse Gray transformation is useful in deciding these spatial relationships. The result of this procedure for $\epsilon = 0.1$ of the 2-element lattice (6) is listed in Table I and shown graphically in Fig. 2(b) for words up to $m = 5$.

To see the utility of Table I, consider the problem of locating all period-2 orbits of (6) for $\epsilon = 0.1$. In sequence space points belonging to period-m orbits are represented by sequences comprised of infinitely repeating m-block words. We use a bar to denote infinite repetition, so that $\overline{01}$ and its shift $\overline{10}$ represent one possible period-2 orbit. In a four symbol alphabet there are exactly six such pairs: $(\overline{01}, \overline{10})$, $(\overline{02}, \overline{20})$, $(\overline{03}, \overline{30})$, $(\overline{12}, \overline{21})$, $(\overline{13}, \overline{31})$, and $(\overline{23}, \overline{32})$. The first two are inadmissible because they contain the forbidden words 010, 101, 020, and 202 listed in line 3 of the table. The other period-2 orbits do not contain any of the forbidden words, nor are they members of the kneading curve. Figure 3 displays the locations of these allowable period-2 orbits computed with the first seven terms of (3).

Computing the kneading curve and evaluating (3) as described above is feasible for small N when symmetry is exploited. For large N an alternate approach would be to compile a lookup table of observed symbol sequences and their locations in state space from time series data, as is done in experimental studies of symbolic dynamics [11–14]. For many coupling geometries the most compact representation would be in terms of the local symbolic dynamics, rather than with symbols describing the global

TABLE I. Forbidden m-block words for $\epsilon = 0.1$.

m	Forbidden m-block words
1	None
2	None
3	010, 020, 100, 101, 102, 110, 111, 120, 122, 200, 201, 202, 210, 211, 220, 222, 310, 320
4	0011, 0022, 0113, 0223, 1031, 1032, 1033 1132, 1231, 2031, 2032, 2033, 2132, 2231 3011, 3022, 3113, 3223
5	00123, 00213, 01123, 02213, 11230, 11330, 11331, 12130, 12330, 12332, 21230, 21330, 21331, 22130, 22330, 22332, 30123, 30213, 31123, 32213

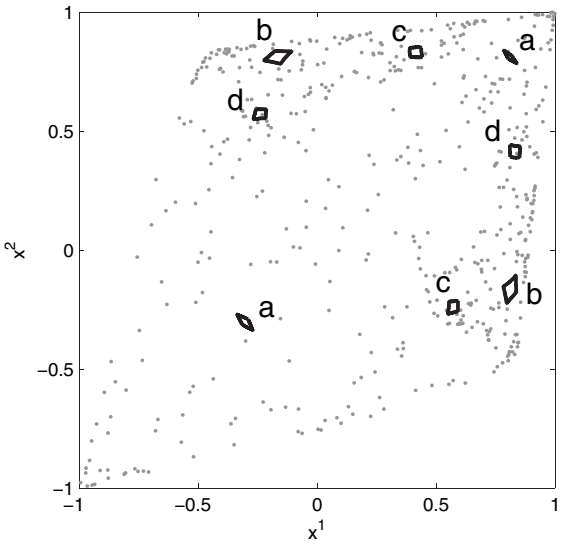

FIG. 3. The locations of the period-2 orbits of the quadratic map CML, Eq. (6), resolved to 7 symbols are overlaid on the attractor (shown in gray). Regions labeled a, b, c, and d correspond to sequences 030 303 0, 121 212 1, 131 313 1, and 232 323 2, and their shifts, respectively.

state. We intend to address the subject of local symbols in future research.

In summary, we present a method for efficiently describing the $\mathbb{R}^N$ dynamics of a broad class of CMLs using N-bit symbols. We show that the concepts of generating partitions and kneading sequences for unimodal maps can be extended to the case of CMLs when the coupling matrix is invertible. The symbolic model can be computed exactly from the images of the generating partition or compiled from time series data. Importantly, these models are useful in chaos control and communication as reported previously [10–16]. Accordingly, we claim that symbolic dynamics provides a natural coordinate system for understanding turbulence in coupled map lattices.

[1] K. Kaneko, *Formation, Dynamics, and Statistics of Patterns*, edited by K. Kawasaki *et al.* (World Scientific, Singapore, 1990).

[2] B. P. Kitchens, *Symbolic Dynamics* (Springer, New York, 1998); B.-L. Hao and W.-M. Zheng, *Applied Symbolic Dynamics and Chaos* (World Scientific, Singapore, 1998).

[3] R. Badii and A. Politi, *Complexity: Hierarchical Structures and Scaling in Physics* (Cambridge University Press, Cambridge, England, 1997).

[4] L. A. Bunimovich and Ya. G. Sinai, Nonlinearity **1**, 491 (1988).

[5] B. Fernandez and P. Guiraud, Discrete Contin. Dynam. Sys. Ser. B **4**, 435 (2004); B. Fernandez and M. Jiang, Ergod. Theory Dyn. Syst. **24**, 107 (2004); W. Just, J. Stat. Phys. **90**, 727 (1998); **105**, 133 (2001).

[6] L. A. Buminovich, Physica (Amsterdam) **103D**, 1 (1997).

[7] Y. B. Pesin and Y. G. Sinai, Advances in Soviet Mathematics **3**, 165 (1991).

[8] V. M. Gundlach and D. A. Rand, Nonlinearity **6**, 165 (1993).

[9] F. H. Willeboordse, Phys. Rev. E **65**, 026202 (2002).

[10] E. Bollt and E. Kostelich, Phys. Lett. A **245**, 399 (1998).

[11] N. J. Corron, S. D. Pethel, and K. Myneni, Phys. Rev. E **66**, 036204 (2002).

[12] N. J. Corron and S. D. Pethel, Phys. Lett. A **313**, 192 (2003).

[13] S. D. Pethel, N. J. Corron, Q. R. Underwood, and K. Myneni, Phys. Rev. Lett. **90**, 254101 (2003).

[14] S. Hayes, C. Grebogi, and E. Ott, Phys. Rev. Lett. **70**, 3031 (1993).

[15] E. Bollt, Y.-C. Lai, and C. Grebogi, Phys. Rev. Lett. **79**, 3787 (1997).

[16] E. Bollt, Int. J. Bifurcation Chaos Appl. Sci. Eng. **13**, 269 (2003).

[17] K. Kaneko, Prog. Theor. Phys. **74**, 1033 (1985).

[18] J. Milnor and W. Thurston, *On Iterated Maps of the Interval I and II* (Princeton University Press, Princeton, 1977).

[19] P. Collet and J.-P. Eckmann, *Iterated Maps on the Interval As Dynamical Systems* (Birkhauser, Boston, 1980).

[20] W. de Melo and S. van Strein, *One-Dimensional Dynamics* (Springer-Verlag, Berlin, 1992).

[21] R. L. Devaney, *An Introduction to Chaotic Dynamical Systems* (Addison-Wesley, Reading, MA, 1989), II ed.

[22] W. Press, S. Teukolsky, W. Vetterling, and B. Flannery, *Numerical Recipes in C* (Cambridge University Press, Cambridge, England, 1992). See section 20.2.

[23] R. H. Abraham, L. Gardini, and C. Mira, *Chaos in Discrete Dynamical Systems* (Springer-Verlag, Berlin, 1997).

[24] P. Cvitanovic, G. H. Gunaratne, and I. Procaccia, Phys. Rev. A **38**, 1503 (1988); K. Hansen, Chaos **2**, 71 (1992); R. Hagiwara and A. Shudo, J. Phys. A **37**, 10 545 (2004); K. T. Hansen and S. Güttler, J. Phys. A **30**, 3421 (1997); H. R. Dullin, J. D. Meiss, and D. G. Sterling, nlin.CD/0408015.